

Experiment Neutrino-4 on search for sterile neutrino at SM-3 reactor

A.P. Serebrov¹, V.G. Ivochkin¹, R.M. Samoilov¹, A.K. Fomin¹, A.O. Polyushkin¹,
V.G. Zinoviev¹, P.V. Neustroev¹, V.L. Golovtsov¹, A.V. Chernyj¹, O.M. Zhrebtsov¹,
M.E. Chaikovskii¹, V.P. Martemyanov², V.G. Tarasenzov², V.I. Aleshin², A.L. Petelin³,
A.L. Izhutov³, A.A. Tuzov³, S.A. Sazontov³, M.O. Gromov³, V.V. Afanasiev³, M.E. Zaytsev^{1,4},
D.K. Ryazanov⁴

1. NRC "KI" Petersburg Nuclear Physics Institute, Gatchina,
2. NRC "Kurchatov institute", Moscow,
3. JSC "SSC RIAR", Dimitrovgrad, Russia,
4. DETI MEPhI, Dimitrovgrad, 433511 Russia

Abstract

The experiment "Neutrino-4" started in 2014 on a model, then it was continued on a full-scale detector, and now, for the first time in the world, has provided the measurement result on dependence of the flux of reactor antineutrinos on the distance of 6 -12 meters from the center of the reactor. One of the main problems, the experiment of "Neutrino-4" faced in carrying out measurements on SM-3 reactor, is the correlated background from fast neutrons caused by space radiation. The reason is that the building with an experimental installation is located on the Earth's surface, and above the installation, there is no sufficiently thick concrete protection. Attempts to suppress the background of fast neutrons by sectioning the detector have given the required result. The relation of effect/background has improved from 0.3 to 0.6. Thanks to sectioning of the detector and use of criterion of an additional event selection, we managed to lower the background of an accidental coincidence, which negatively influenced the accuracy of measurement. As a result, measurements of the difference in the counting rate of neutrino-like events (reactor ON–reactor OFF) for a full-scale detector have been obtained as dependence on distance from the reactor center. Besides, the spectrum of prompt signals of neutrino-like events has been presented. Comparison with Monte Carlo simulation spectrum is performed applying antineutrino spectrum for U²³⁵, because the SM-3 reactor uses highly enriched uranium. The fit of experimental dependence with the law $1/L^2$, however, does not give an absolutely satisfactory result. The goodness of that fit is a little more than 10%, i.e. the confidence level is about 90% in deviation from the law $1/L^2$ (1.64σ). The similar situation arises in the analysis of spectrum dependence of prompt signals, which is also 90% of confidence level. Of course, the joint deviation, demanding identical parameters $\Delta m_{14} \approx 0.7 \div 0.8 eV^2$ and $\sin^2 2\Theta_{14} \approx 0.10 \div 0.15$, increases the confidence level up to about 95% (2σ). But it is still not enough for making statements on observation of the phenomenon, especially, such an important one as oscillations in a sterile state. At last, it is also impossible now to exclude possibility of influence of systematic errors on the final experimental result. Therefore, in future we would like to concentrate efforts on increase in accuracy of the experiment and control of possible systematic errors. The scheme of a new experiment is under consideration.

Introduction

At present, there is a widely spread discussion on possible existence of a sterile neutrino having much less cross-section of interaction with matter than, for example, a reactor electron antineutrino. It is assumed, that owing to a reactor antineutrino transition to a sterile state, the oscillation effect at a short reactor distance and deficiency of a reactor antineutrino flux at a long range are likely to be observed [1, 2]. Moreover, a sterile neutrino can be considered as a candidate for the dark matter.

Ratio of the neutrino flux observed in experiments to the predicted one is estimated as 0.927 ± 0.023 [1]. The effect comprises 3 standard deviations. This is not yet sufficient to have confidence in existence of the reactor antineutrino anomaly. The method for comparing the measured antineutrino flux with the expected one from the reactor is not satisfactory, because of the problem of accurate estimating a reactor antineutrino flux and efficiency of an antineutrino detector. In fig. 1 is shown a possible process of oscillations to a sterile state at small distances from an active zone of the reactor, which is presented in work [1].

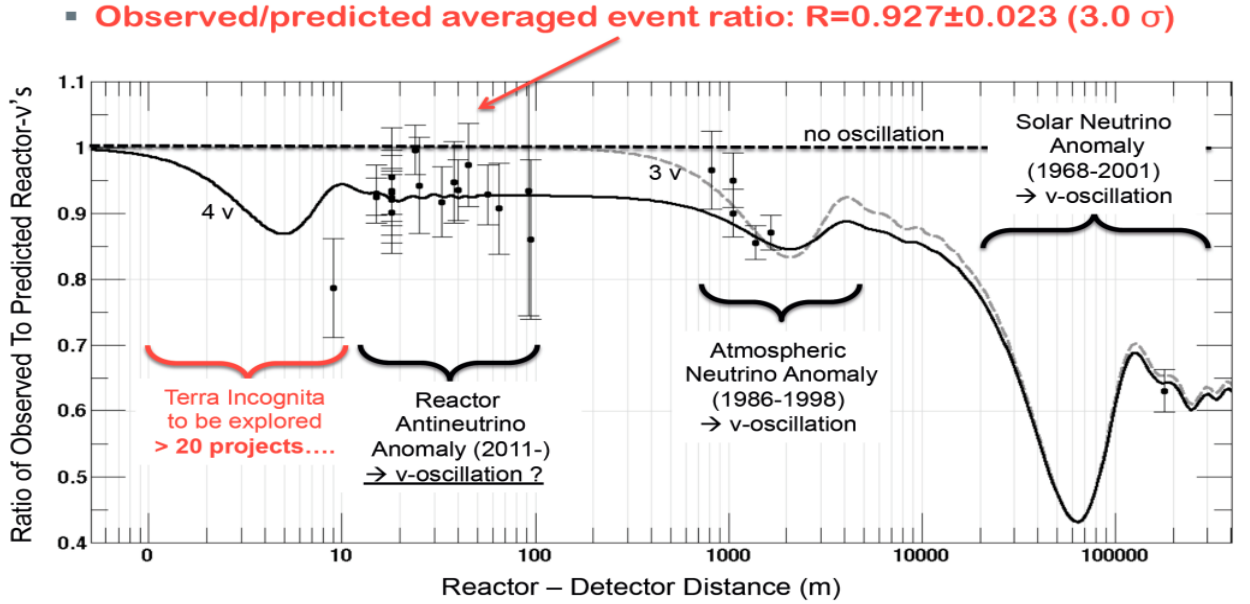


Fig.1 The possible process of oscillations to a sterile state at small distances from an active zone of the reactor presented in [1].

The idea of oscillation can be verified by direct measuring of a flux distance dependence and antineutrino spectrum at a short reactor distance of 6 – 12m. A detector is supposed to be movable and a spectrum sensitive. Our experiment focuses on the task of confirming possible existence of a sterile neutrino at a certain confidence level, or disproving it. For searching oscillations to a sterile neutrino, it is necessary to register discrepancy of the reactor antineutrino flux. If such a process does occur, it can be described by an oscillation equation:

$$P(\tilde{\nu}_e \rightarrow \tilde{\nu}_e) = 1 - \sin^2 2\theta_{14} \sin^2 \left(1.27 \frac{\Delta m_{14}^2 [\text{eV}^2] L [\text{m}]}{E_{\tilde{\nu}} [\text{MeV}]} \right) \quad (1),$$

where $E_{\tilde{\nu}}$ is antineutrino energy, with oscillations parameters Δm_{14}^2 and $\sin^2 2\theta_{14}$ being unknown.

For the experiment to be conducted, one needs to make measurements of the antineutrino flux and spectrum at short distances of 6-12 m from, practically, a point source of antineutrino.

We have studied opportunities for making new experiments at research reactors in Russia. The research reactors should be employed for performing such experiments, since they possess a compact reactor core, so that a neutrino detector can be placed at a sufficiently small distance from it. Unfortunately, the research reactor beam hall has quite a large background of neutrons and gamma quanta, which makes it difficult to perform low background experiments. Due to some peculiar characteristics of its construction, reactor SM-3 provides the most favorable conditions for conducting an experiment on search for neutrino oscillations at short distances. Unfortunately, SM-3 reactor is located on the Earth surface, hence, cosmic background is the major difficulty in making such experiments by research reactors.

1. Reactor SM-3.

Initially, 100-megawatt reactor SM-3 was designed for carrying out both beam and loop experiments. Five beam halls were built, separated from each other with big concrete walls as wide as ~ 1 m (Fig. 2). This enabled to carry out experiments on neutron beams, without changing background conditions at neighboring installations. Later on, the main experimental program was focused on the tasks concerned with irradiation in the reactor core center. For 25 years of exploitation, a sufficiently high fluence was accumulated on materials of the reactor cover, which necessitated its replacement. Setting a new reactor cover on new reactor tank was the simplest way to solve this problem. Such a solution, however, resulted in raising a reactor core center by 67 cm higher than in the previous position.

Reactor: SM-3 reactor in Dimitrovgrad (Russia): 100 MW compact core $35 \times 42 \times 42 \text{ cm}^3$

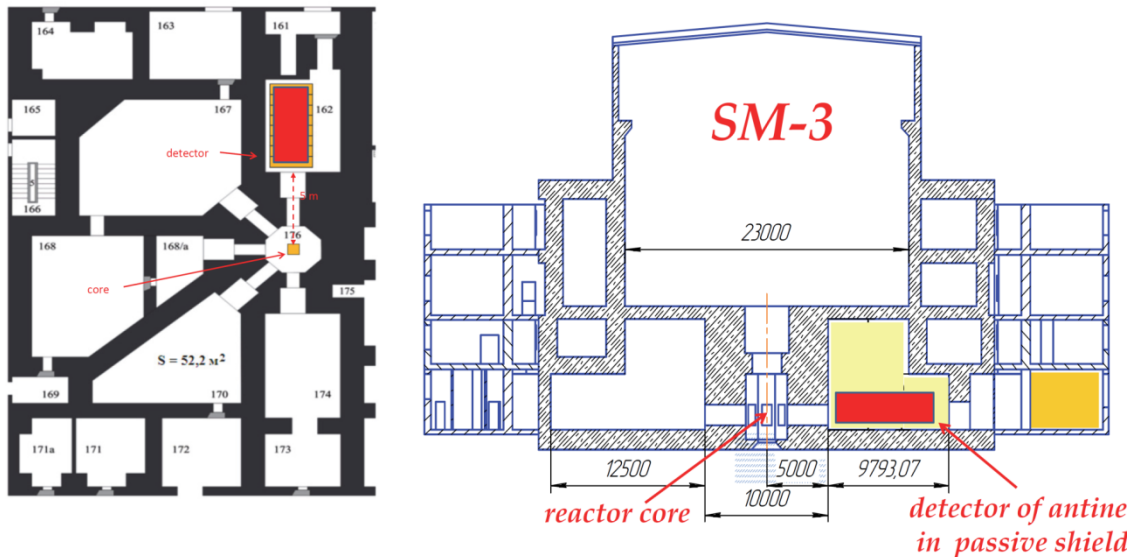


Fig.2. Detector location at reactor SM-3: 1 – reactor core, 2 – antineutrino detector.

Horizontal beam channels were removed, as priority was given to conducting loop experiments. Neutron flux in the location of the former beam channels was lowered by four orders of magnitude. Respectively, it caused decrease in the neutron background to about $4 \cdot 10^{-3} \text{ n}/(\text{cm}^2 \cdot \text{s})$ (on thermal neutrons) in the former beam halls. It is approximately by 4 – 5 orders of magnitude lower than a typical neutron background in the beam hall of a research reactor.

Lately, in making preparations for an experiment on search for oscillations of a reactor antineutrino to a sterile state at reactor SM-3, upgrading of a slide valve of the former neutron beam has been completed. As a result, the background of fast neutrons has diminished to the level of $10^{-3} \text{ n/(cm}^2\text{s)}$, i.e. practically, to the level of neutron background on the Earth surface, caused by space radiation. These conditions are most preferable of all possible for a neutrino experiment to be performed. Other advantages of SM-3 reactor are a compact reactor core center ($35 \times 42 \times 42 \text{ cm}$), with high reactor power equal to 100 MW, as well as a sufficiently short distance (5 m) from the center of a reactor core to the walls of an experimental hall. Besides, of special significance is the fact that antineutrino flux can be measured within a sufficiently wide range from 6 to 12 meters. Up to $1.8 \cdot 10^3$ neutrino events are expected to occur per day, at the reactor power 100 MW, at distance of 6 m from the reactor core center, within the volume of 1 m^3 . Hence, considering registration efficiency to be about 20% , with 400 liters of liquid scintillator, we can record about 150 neutrino events per day. This statistics level is not very high, so the cosmic background remains the major problem of the experiment.

2. Passive shielding of a neutrino detector at SM-3 reactor.

Layout of passive shielding (“cabin”) from the outside and inside is given in Fig. 3. It is created from elements based on steel plates of $1 \times 2 \text{ m}$, 10mm thick, to which are attached 6 lead sheets of 10 mm thickness. The cabin volume is $2 \times 2 \times 8 \text{ m}$. From the inside, the cabin is covered with plates of borated polyethylene of 16 cm thickness. The total weight of passive shielding is 60 tons, the volume of borated polyethylene is 10 m^3 . Inside the passive shielding, there is a platform with an antineutrino detector, which can be moved along the rails within the range 6 - 12 meters from the reactor core center. A neutrino channel can be entered by means of a ladder, through the roof with the removed upper unit, as shown in Fig. 3. Loading of the detector into a neutrino channel is carried out from the main hall, through a trap door in the building ceiling. In this case, an overhead crane of the main hall is used.



Fig.3. General view of passive shielding: from the outside and inside. The range of detector dislocation is 6 - 12 m from the reactor core center.

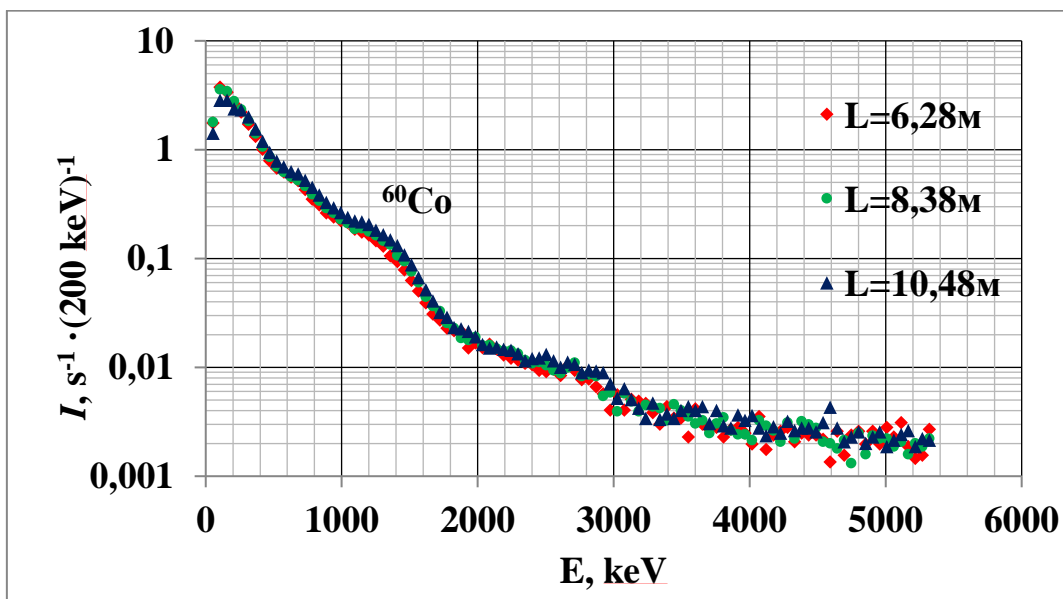
3. Investigation of background conditions with a gamma detector from the inside of passive shielding for an experiment Neutrino-4.

For measuring the gamma ray spectrum, a detector NaJ(Tl) of 60×400 mm was applied. In switching on the reactor, it shows counts of gamma-quanta from a neutron capture in an iron-concrete shielding of the reactor. During a reactor operation, the background of gamma radiation, in the energy range from 3 MeV to 8 MeV significantly increase (22 times larger than reactor Off state), because of thermal neutrons interaction with iron nuclei in construction materials. This energy range is of great importance, since it corresponds to gamma-quanta energy at the neutron capture by Gd.

Gamma-radiation of isotopes ^{137}Cs , ^{60}Co is independent of the reactor operation mode and is caused by radioactive contamination from the building floor and walls. In spite of pouring of the concrete floor with iron grit and reconstruction of a slide valve, which reduced 5 - 6 times gamma radiation background in this energy range, it does remain high enough, which confirms necessity of passive shielding from gamma quanta for a detector.

Within energy range of 1440÷7200 keV (from ^{40}K and higher), the 5 cm lead shielding makes the level of background gamma radiation 4.5 times lower, which proves that its installation on the detector is reasonable. However, it is to be noted, that neutron background, resulting from the interaction of cosmic muons with lead nuclei, enhances inside the lead shielding. Indeed, the 5 cm lead shielding around a neutron detector results in raising twice its count rate. Hence, inside the lead shielding, there must be located another one, made from borated polyethylene.

Fig. 4 presents the gamma spectrum shape inside the passive shielding for different distances along the way of a neutrino detector: 6.28 m, 8.38 m, 10.48 m. No noticeable alterations in the spectrum shape is observed. Moreover, for comparison, gamma-spectra are measured at the reactor On and Off inside the passive shielding, at the point nearest to the reactor. Considerable difference in spectra is not found.



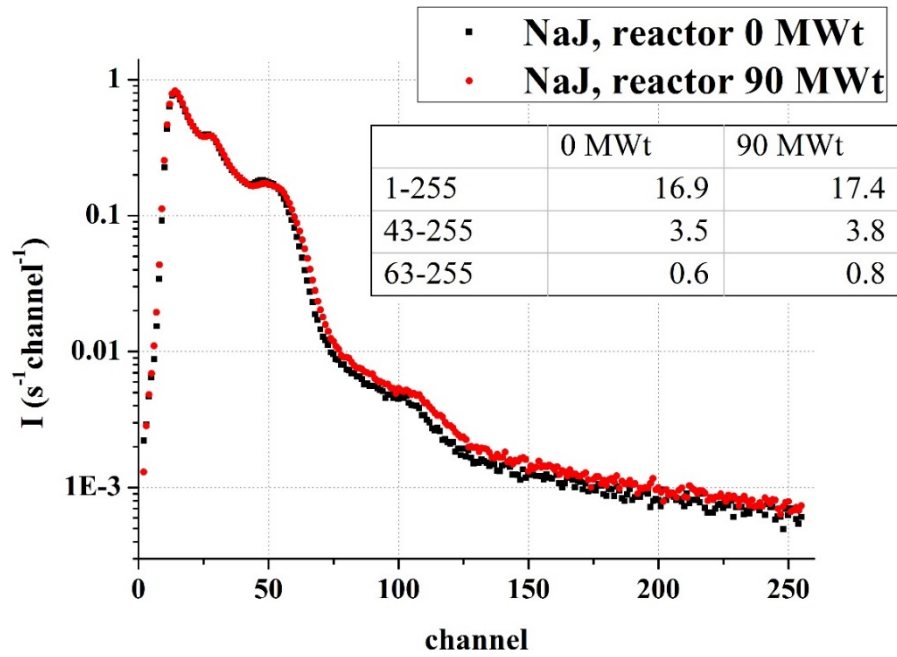


Fig.4. Gamma-radiation spectra at the detector location. a) Reactor power is 90MW. L is distance from the reactor core center: - 6.28 m, - 8.38m, - 10.48m. b) Reactor ON/OFF spectra.

4. Estimations of the fast and thermal neutron fluxes by a neutron detector in the neutrino laboratory building and inside the passive shielding.

In 2013, at SM-3 reactor, a neutrino laboratory building was completed for exploitation and the equipment for passive shielding of a neutrino detector was mounted. The slide valve for the former neutron channel was carefully plugged. As a result, a flux of thermal neutrons in the neutrino laboratory building decreased 29 times to the level of $1 \div 2 \cdot 10^{-4} \text{ n/cm}^2 \cdot \text{s}$. This level is determined by space radiation neutrons and, practically, is independent of the reactor operation. Measurements of thermal neutron fluxes were made with ^3He detector, which is a proportional counter of 1m long with diameter of 30 mm. For registration of fast neutrons, we used the same proportional ^3He detector, but it was put into the shielding made of polyethylene (thickness of layer is 5 cm), which in its turn was wrapped in a layer of borated rubber (3 mm thick, containing 50% of boron). To convert count rate (s^{-1}) of proportional ^3He detector into density units of a prompt neutron flux ($\text{cm}^{-2} \cdot \text{s}^{-1}$), a newly created fast neutron detector was calibrated according to recordings of standard MKC AT6102. For this purpose both detectors were placed side by side at distance of 3 m from a neutron source (Pu-Be). Thermal neutrons detector was calibrated in the same way. Made in this way, detectors of thermal and fast neutrons have sensitivity nearly by two orders of magnitude higher than that of standard devices. They were employed for conducting low-background measurements by a neutrino laboratory. Estimations on neutron background were made, at first, before gate upgrading of the former neutron beam (before slide valve was plugged), then, after upgrading and, finally, after installing passive shielding for a neutrino detector. A detector of fast neutrons was located on the roof of passive shielding and

directly on the reactor wall, i.e. at distance of 5.1 m from the reactor core center. Measurements results are presented in in Fig.5.

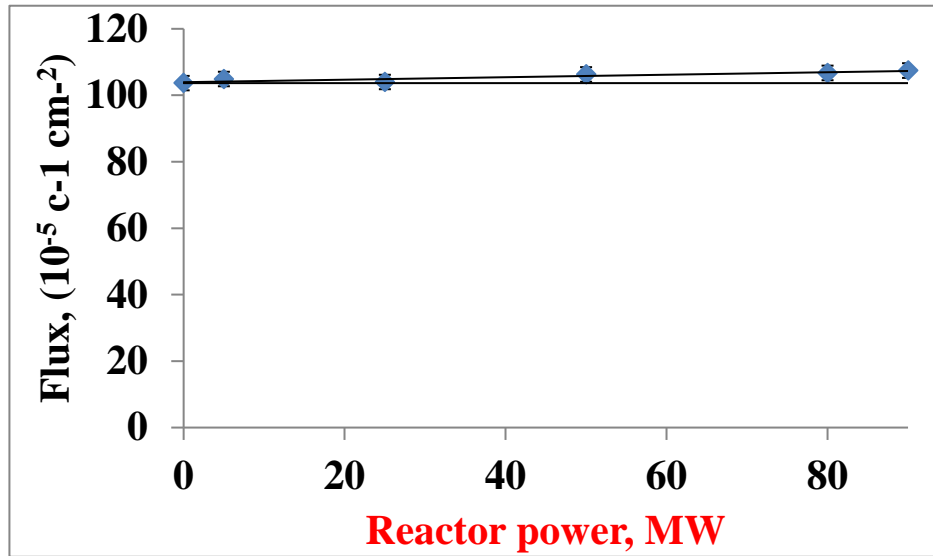


Fig.5. Flux of a fast neutron detector at the output of a power reactor 90MW. The counter is located on the cabin roof at the reactor wall.

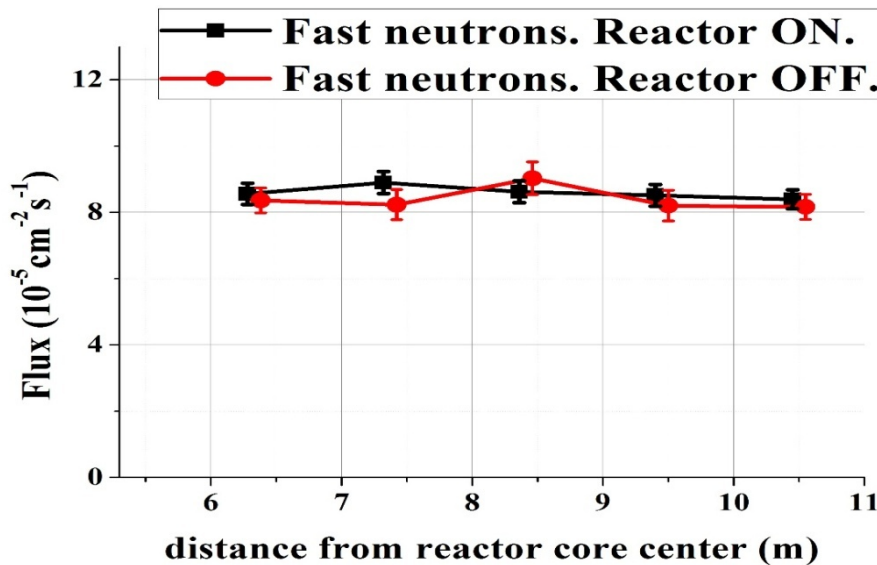


Fig.6. Fast neutron background at different distances from the reactor core center measured with the detector of fast neutrons inside passive shielding.

The fast neutron detector was set on the cover of the neutrino detector and dislocated together with it. From Fig.5, one can conclude that background of fast neutrons, practically, does not depend on the reactor power. It is determined by neutrons emerging from interaction of muons with nuclei of the surrounding materials, in particular, with lead nuclei of passive shielding. However, suppression of the flux with internal lining of passive shielding (16 cm of borated polyethylene) is 12 times higher.

Another problem of great significance is reactor influence on the flux of fast neutrons inside passive shielding. Measurements of the fast neutron flux inside passive shielding at reactor On were in progress, at the nearest to the reactor wall, for about ten days, and for the same time after switching it off. At the reactor On the fast neutron flux was equal to $(5.54 \pm 0.13) 10^{-5} \text{ s}^{-1} \text{ cm}^{-2}$,

while at the reactor Off, it was $(5.38 \pm 0.13) 10^{-5} \text{ s}^{-1} \text{ cm}^{-2}$, i.e. there was no difference within the accuracy of 2.5%.

Much more detailed measurements were made with a fast neutron detector on the cover of a neutrino detector, moved during these measurements along the neutrino channel in the range from 6.25 m to 10.5 m. Results of these measurements at the reactor On and the reactor Off are given in Fig. 6. There is no difference in results at the reactor On and the reactor Off within statistical estimation accuracy. The background involved is determined by space radiation. In these measurements, the background level appeared to be equal to $(8.5 \pm 0.1) 10^{-5} \text{ s}^{-1} \text{ cm}^{-2}$, which is somewhat higher than that at the reactor wall. The discrepancy can result from the detector location regarding the direction of a neutron flux, i.e. its vertical position at the reactor wall as well as a horizontal one, on the cover of the neutrino detector.

5. Investigation of background conditions with a neutrino detector model.

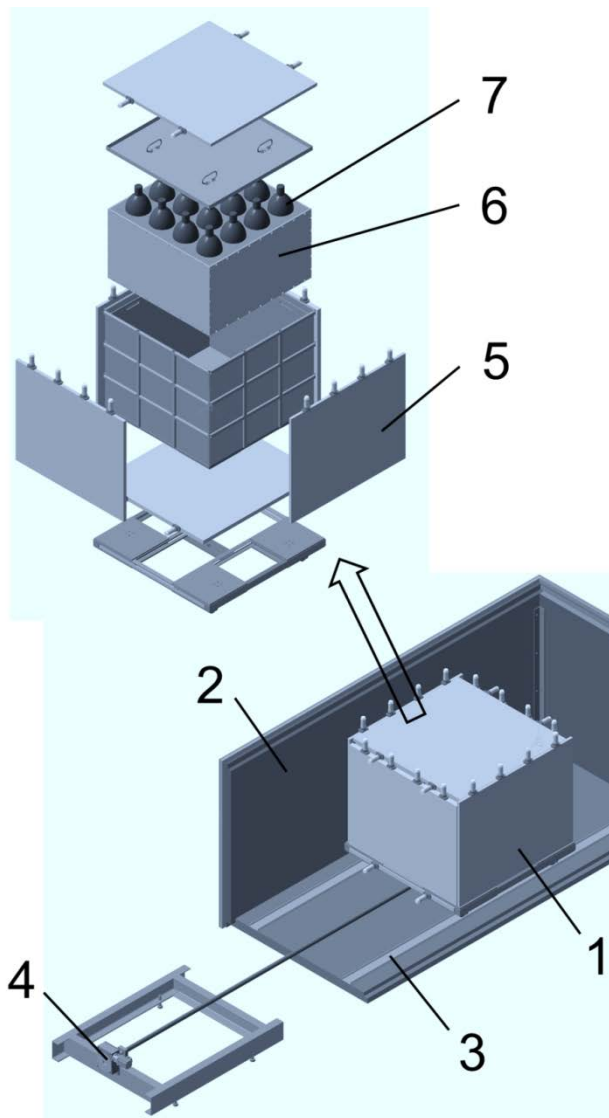


Fig7. Model of the neutrino detector installed in passive shielding [4].

- 1 – detector of reactor antineutrino,
- 2 – passive shielding,
- 3 – rail,
- 4 – engine for detector movement,
- 5 – active shielding with PMT,
- 6 – volume with liquid scintillator with Gd (~ 400 l),
- 7 – Detector's PMT.

A neutrino detector model contains 400 l of liquid scintillator BC-525 with 1 g/l of Gd concentration, 16 PMT on the top and 5 active shielding(muon veto) around.

Fig. 8 shows neutrino detector model spectrum to be conventionally divided into 4 parts. The first part of it (up to 2 MeV) is relevant to the radioactive contamination background, the second one (from 2 MeV to 10 MeV) covers the neutron registration area, since it corresponds to gamma-quanta energy at neutron capture by Gd. The range from 10 to 60 MeV is related to a space radiation soft component produced by muon decay and muon capture in substance. And finally, the range from 60 – 120 MeV is related to a muon component passing through the detector. Here are also shown small alterations of the spectrum shape for different detector positions.

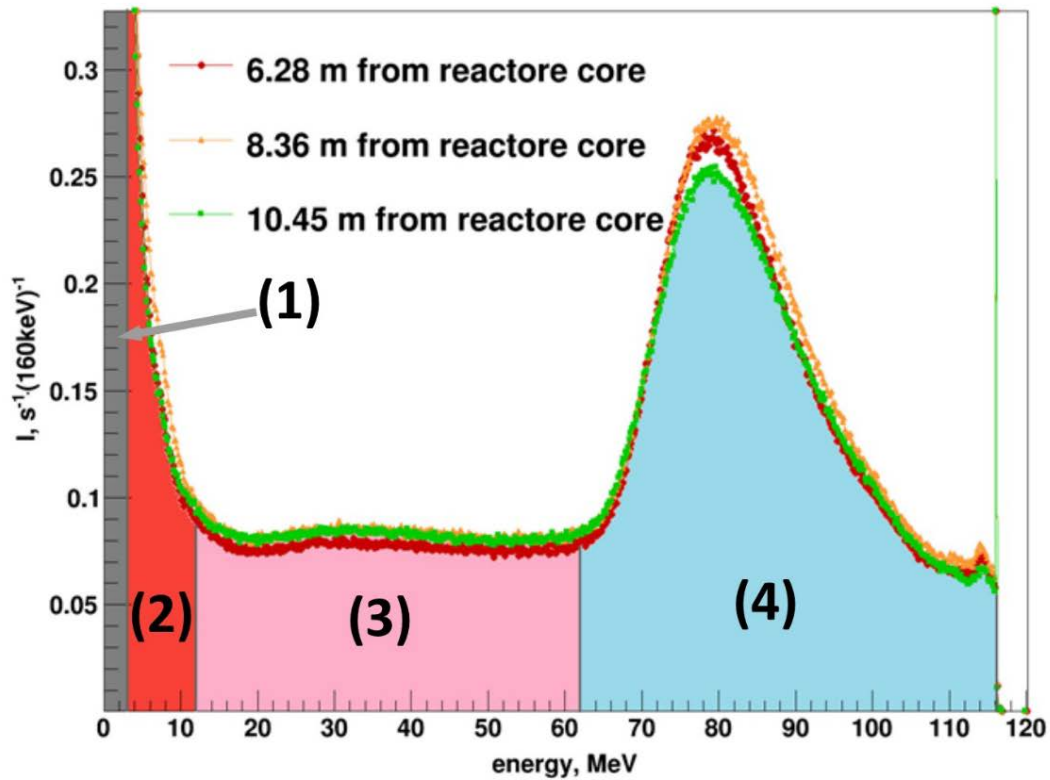


Fig.8. Detector energy spectrum at different distances from the reactor core center and a conventional division of spectrum into zones: 1 – radioactive contamination background, 2 – neutrons, 3 – space radiation soft component, 4 –muons.

In the course of long-term measurements, temporal variations of cosmic radiation intensity have been found. They are caused by fluctuations of atmospheric pressure and some temperature drift during season changes. It is a well known barometric and temperature effect of cosmic rays [5,6]. Muons are formed in the upper layers of atmosphere. Higher pressure gives rise to a larger amount of substance over the detector and to intensity attenuation of cosmic rays. Fig. 9 shows anti-correlation effect between the atmospheric pressure and the total intensity of fast and slow components of space radiation, i.e. within the energy range from 10 to 120 MeV. This is the barometric effect. Behavior of fast and slow components is distinguished by presence of an additional long-term drift, with the drift sign being opposite for fast and slow components. It is so called temperature effect which can be interpreted in the following way. At the rise of the temperature in lower atmospheric layers, their expansion increases the layer responsible for formation of muon fluxes. As the distance to the Earth grows, the share of the decayed muons is getting larger. Thus, the intensity of fast component (muons) decreases and that of slow component (products of decay: electrons, positrons, gamma quanta) rises. Fig.10 shows a drift

effect with opposite signs for fast and slow components of space radiation at higher temperature of the lower layers of atmosphere in the vicinity of the Earth surface since January till April: from -30°C to $+10^{\circ}\text{C}$.

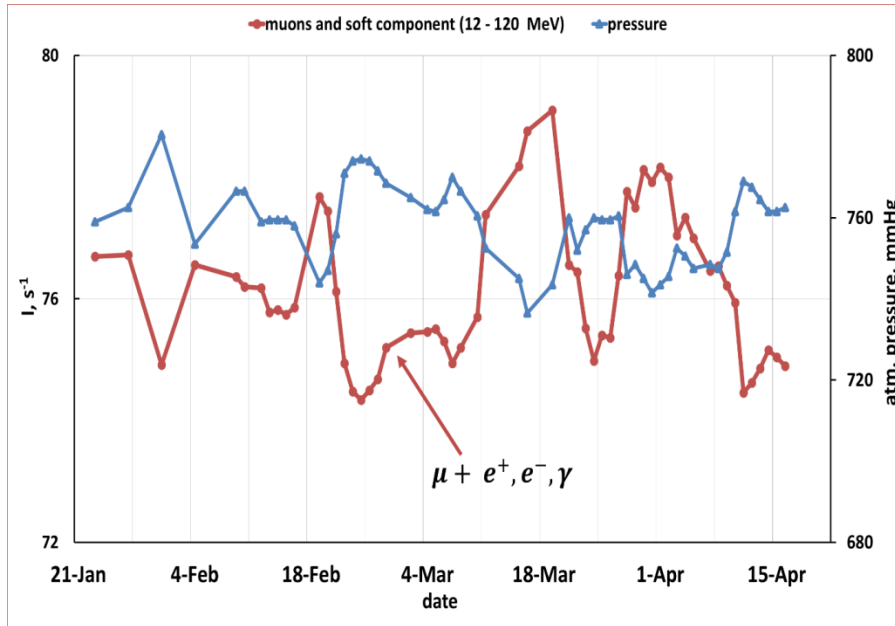


Fig.9. Barometric effect of cosmic rays: the left axis illustrates a summary detector count rate in the area of 3 and 4, the right axis shows atmospheric pressure, the horizontal axis gives the measurement time since 23 of January till 15 of April of 2014.

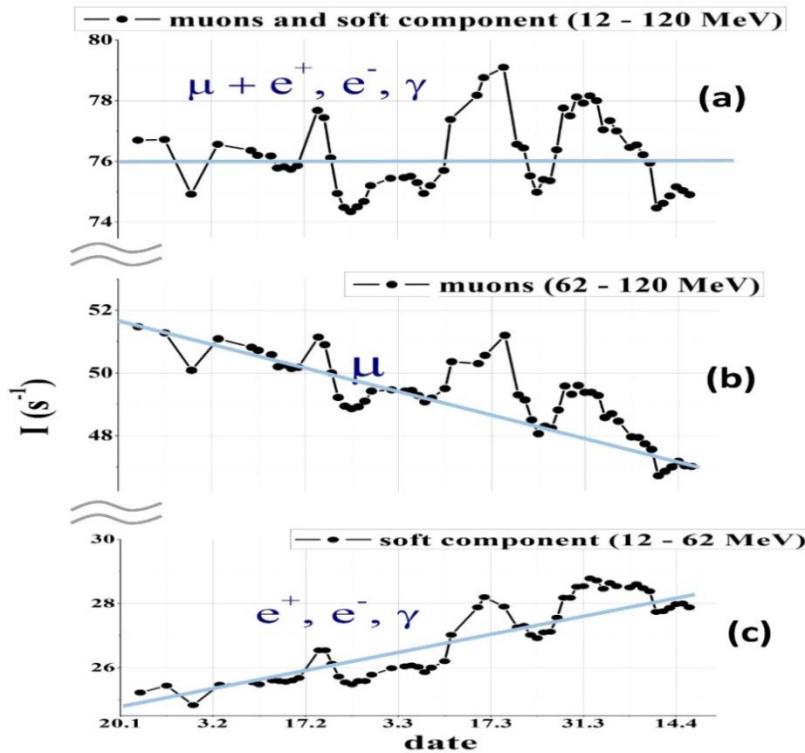


Fig.10. Barometric and temperature effects of cosmic rays: a) a summary detector count rate in the area of 3 and 4, b) a detector count rate in the area of 4, c) a detector count rate in the area of 3. Along the horizontal axis is the measurement time since 23 January till 15 April of 2014.

6. Energy and Time Spectra of Correlated Events.

As it was noted earlier, in measuring antineutrino flux from the reactor, the technique of correlated coincidences is employed for distinguishing the registration process of antineutrino - $\bar{\nu}_e + p \rightarrow e^+ + n$. Fig. 11 gives time spectra of delayed coincidences. The background of accidental coincidences is subtracted. One can see two exponents (straight lines in logarithmic scale), which correspond to a muon decay and a neutron capture by Gd. Without applying active shielding, the integral under the first exponent corresponds to stopped muon count of $1.54 \mu\text{s}$, and the exponent ($2.2 \mu\text{s}$) corresponds to a muon lifetime. The integral under the second exponent is relevant to a neutron capture rate in the detector – 0.15 n/s , and the exponent ($31.3 \mu\text{s}$) corresponds to a neutron lifetime in the scintillator at 0.1% of Gd concentration.

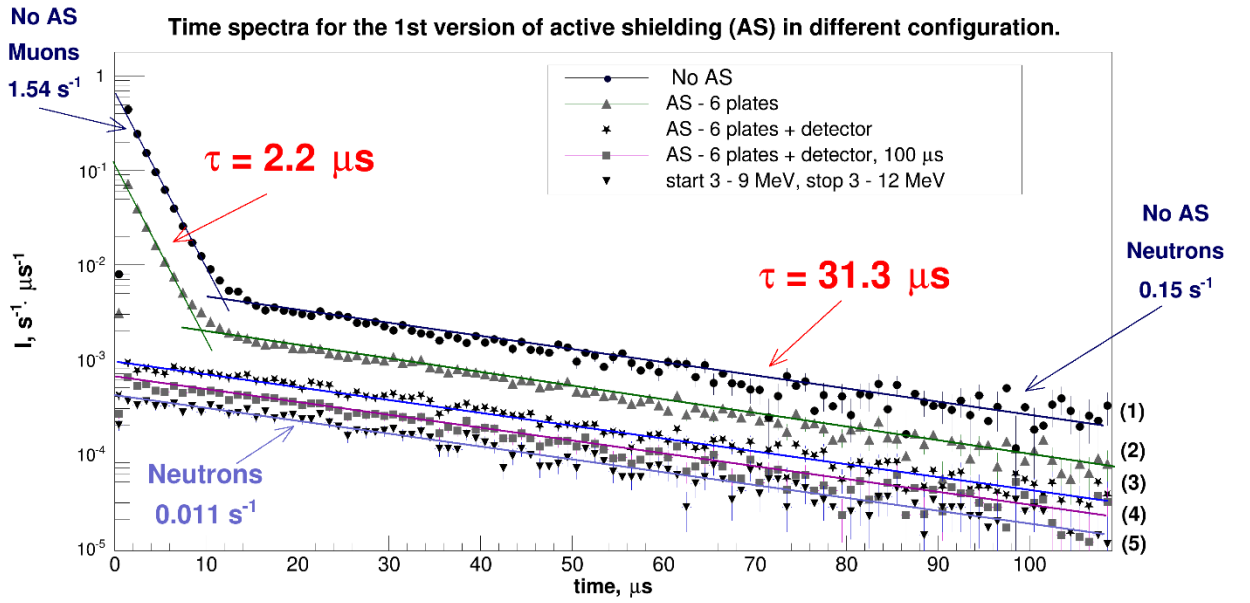


Fig. 11. Time spectra at different configurations of active shielding: 1 - no active shielding, 2 – plates of active shielding are on, 3 – the same + ban from the detector at signals higher than 12 MeV, 4 – the same + ban on 100 μs after the detector signal, at energy higher than 12 MeV, or after the signal in active shielding, 5 – the same + limit on start and stop signals in ranges 3 – 9 MeV and 3 – 12 MeV respectively.

The number of muon stops per second corresponds to the estimation made on the muon flux and the scintillator mass calculation, while the number of captured neutrons per second corresponds to the calculated rate of neutron generation in the detector itself, caused by a muon flux passing through it. It points out that, in general, one succeeded in solving the task under consideration by means of passive shielding in combination with lead placed outside and with 16 cm of borated polyethylene inside. Indeed, addition of the 10 cm borated polyethylene upon the detector cover inside the cabin does not alter a neutron capture rate in the detector. Use of veto from active shielding and the detector, which gives evidence for muon passing, allows to suppress the capture rate by the detector to the level of $1.8 \cdot 10^{-2} \text{ n/s}$. Fig.11 presents results achieved with the first version of active shielding.

The most essential experimental problem is possibility of distinguishing correlated events from the background of accidental coincidences. Fig. 12 presents examples of correlation signal measurements.

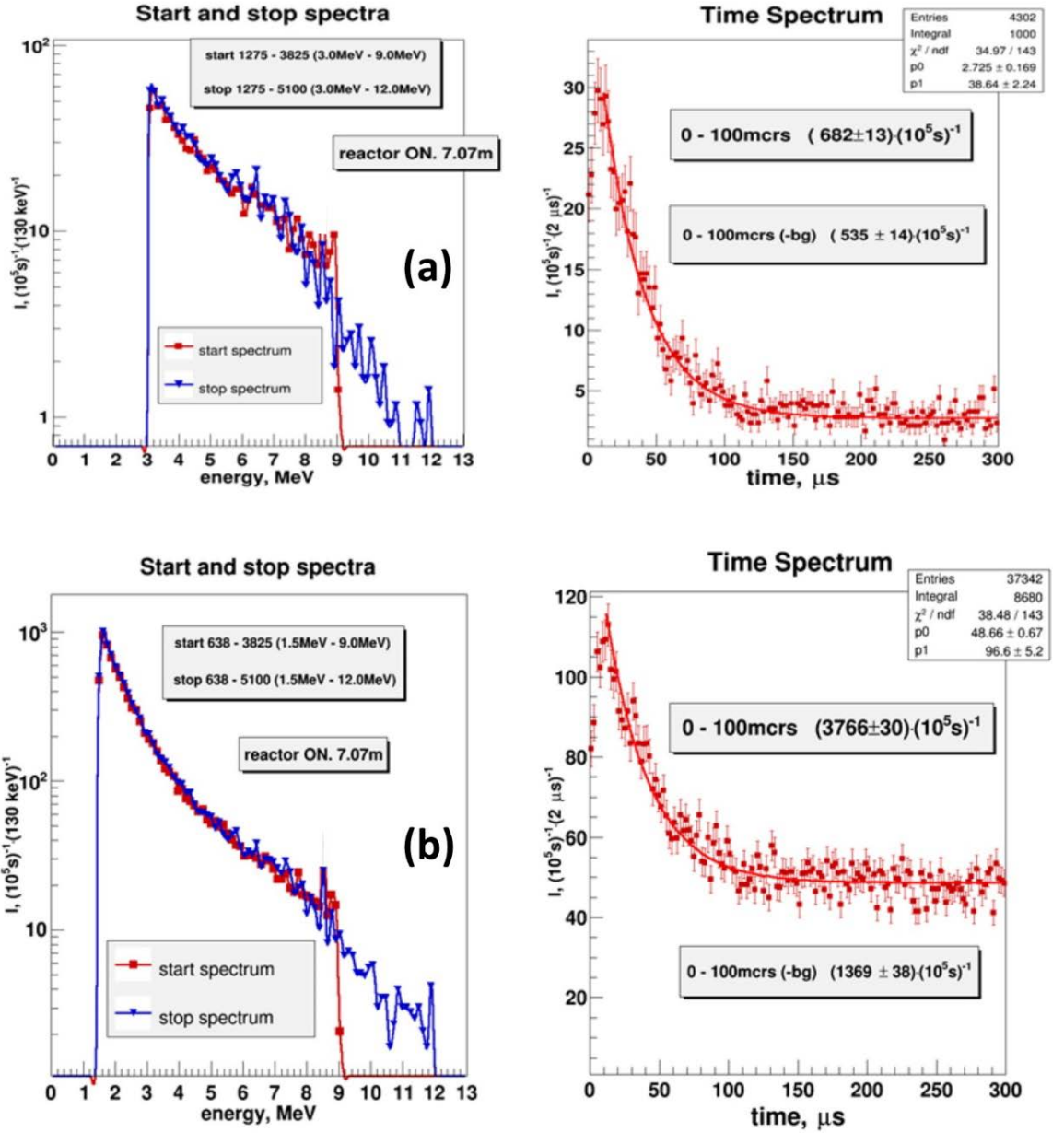


Fig. 12. Energy spectra of prompt and delayed signals and time spectra: a) threshold of start and stop signals 3 – 9 MeV and 3 – 12 MeV respectively, b) 1.5 – 9 MeV and 1.5 – 12 MeV.

Measurements for delayed coincidences were made for 300 μs after prompt signal, the latest 100 μs used for measuring background of an accidental coincidences. At lower threshold of prompt and delayed signals of 3 MeV, contribution of accidental coincidences is very small (Fig. 12a). In decreasing the lower threshold the rate of accidental coincidences increases, however, the number of correlated events grows (Fig. 12b). Nevertheless, statistical accuracy of correlated signal is not growing. Radioactive contamination background remains high enough. Unfortunately, its reduction does not seem to be possible for the time being. However, it should be noted, that a much more essential problem appears to be concerned with correlated background related to space radiation, i.e. muons and fast neutrons.

7. Carrying out research with a model of antineutrino detector of a multi section type.

Creation of a multi section system is aimed at finding criteria for detection of neutrino events. The main problem of an experiment on the Earth's surface is fast neutrons from space radiation. The scattering of fast neutrons easily imitates a neutrino process. Registration of the first (start or prompt) signal from recoil protons imitates registration of a positron. The second (stop or delayed) signal arises in both cases when a neutron is captured by gadolinium. The difference between these prompt signals is in appearance of two gamma quanta from annihilation of a positron from IBD (inverse beta decay) process. Positron range in an organic scintillator is less than 5cm. The recoil proton track with high probability is within the size of one detector section, because length of a recoil proton track is about 1 mm. Gamma quanta with energy of 511 keV can be registered in adjacent sections.

The problem of fast neutrons

Neutrino event

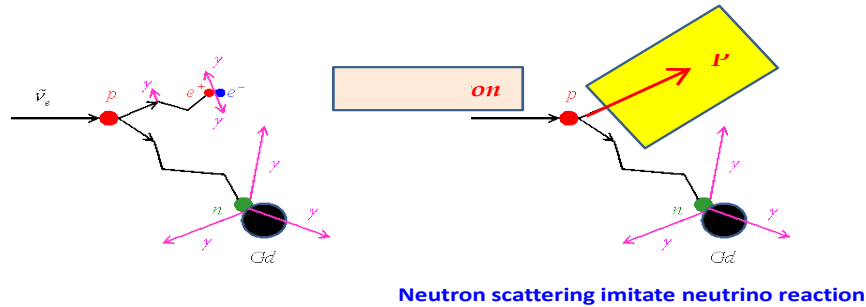


Fig 13. The Illustration of a background problem from fast neutrons.

Unfortunately, 70% of starting signals from neutrino events can be also recorded within one section. Only 30% of neutrino starting signals are multi-sectional due to registration of γ quanta in the sections adjacent to that, in which positron annihilation occurs. Obviously, the suppression of statistics of neutrino events by factor 3 is hardly acceptable, but the analysis of results can be performed by using the single-section and multi section events, and also their sum. The ratio of 30% to 70% is taken for the multi-section and single-section events as a selection criterion for neutrino events. Thus, if signal difference between the reactor ON and reactor OFF measurements is within 30% - 70% for the multi section and single-section events, then it can be interpreted as a neutrino signal. This relation depends on the detector structure, i.e. the size of sections and their number. Therefore, Monte Carlo calculations for this particular structure are necessary.

The detector scheme is presented in fig. 14. It consists of 16 sections of $0.225 \times 0.225 \times 0.5$ m with rigidly fixed partitions between them. Partitions serve to prevent light from leaving section limits. Scintillator material is mineral oil (CH_2) with Gd additive of 1 g/l. The light yield of a scintillator is 10^4 photons on 1 MeV. The air layer between scintillator and PMT allows to improve the section energy resolution, since the effect of a full internal reflection on the surface

of a liquid scintillator reduces a solid angle for the light to be able to leave the zone closest to PMT. Photons have mirror reflections on the walls. Exponential length of photon track in a scintillator is 4 m. Photons are reflected from the walls with probability of 0.95. The probability of registration of double starts, when the major signal corresponds to different detector cells is presented in table 1.

Table 1

central cell, double coincidence	side cell, double coincidence	angular cell, double coincidence	in all cells, double coincidence
0.424	0.294	0.188	0.300

Probability of recording double starts depends on the section location: in the center, on the sides or in the corner. The average probability for the whole detector is 30%. A specified structure of distribution of the double start probability is specific for neutrino events, since it is determined by the process of positron annihilation, during which emission of two gamma quanta with energy of 511 KeV occurs.

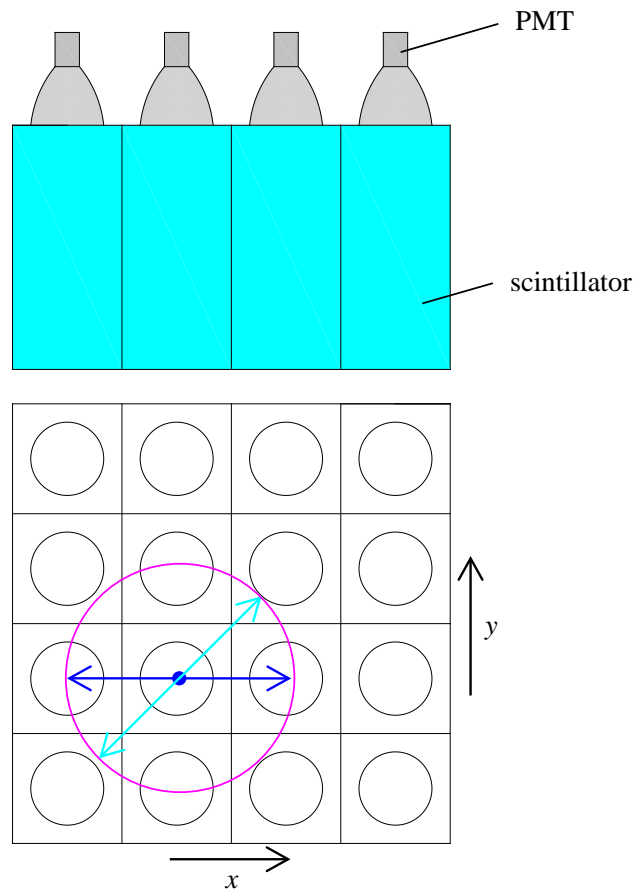


Fig. 14. Scheme of the detector of reactor antineutrinos.

Preliminary measurements with Pu-Be neutron source have been made before the main measurements with a new detector model. The time spectra of the single-section and multi-section prompt signals, and also of their sum is shown in Fig. 15. It appears, that if we consider only multi prompt signals, then the correlated signals from neutrons are completely excluded and only a straight line from an accidental coincidence remains: the blue curve is a sum of green and red curves. This experiment has revealed that fast neutrons give single-section starts.

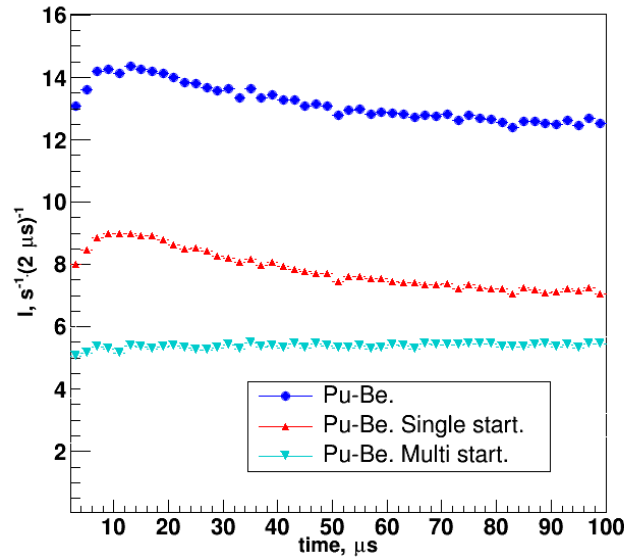


Fig.15 Time spectra of the delayed coincidence obtained with a neutron Pu-Be source. The blue curve corresponds to any starting events, including the single-section and multi-section starts. The red curve corresponds to single-section starts, and the green one shows multi-section starts.

8. Design of a multi-section antineutrino detector model.

The detector inner vessel of $0.9 \times 0.9 \times 0.5 \text{ m}^3$ is filled with a liquid scintillator doped with Gadolinium (0.1%). The detector of a scintillation type is based on IBD reaction: $\bar{\nu}_e + p \rightarrow e^+ + n$. The detector consists of 16 sections $0.225 \times 0.225 \times 0.5 \text{ m}$ with rigidly fixed partitions between them. The detector model was designed as a multi-sectional one in order to distinguish the positrons emitted in an IBD reaction and recoil protons from a fast neutron elastic scattering. Active shielding of a neutrino detector consists of external (“umbrella”) and internal parts relative to passive shielding [7].

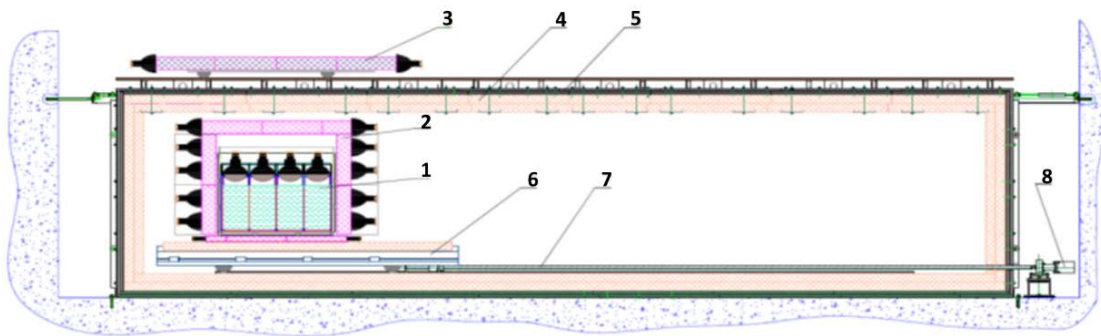


Fig 16. General scheme of an experimental setup: 1 – detector of reactor antineutrino, 2 – internal active shielding, 3 – external active shielding (umbrella), 4 – borated polyethylene passive shielding, 5 – steel and lead passive shielding, 6 – moveable platform, 7 – feed screw, 8 – step motor.

For making measurements the detector can be transported into different positions, with 0.5m distance between them, to avoid the influence of difference in efficiency of different sections. Shifts can be made from one position to any other. The sectioned detector structure allows us to present the distance dependence with 0.5 meter step. The measuring technique makes it possible to move detector for 1 meter, starting with the position closest to reactor. On the second stage, measurements are remade with changing the starting position for 0.5 meters. Thus, both detector sides measure the same points, averaging, in this way, somewhat different registration efficiency of each detector side. The count rate difference (ON-OFF, i.e. with the reactor switched on and off) for two-section and single-section starts, integrated at all distances, makes up $(29\pm7)\%$ % and $(71\pm13)\%$ % respectively. Within the available accuracy, such a ratio allows to assume the registered events as neutrino-like events.

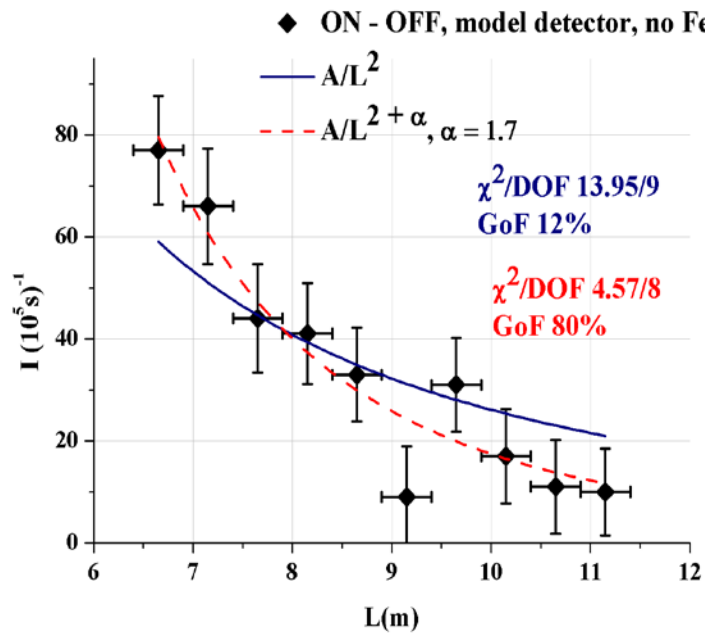


Fig. 17. Count rate difference (ON-OFF) for the delayed coincidence in a time window is $100\mu\text{s}$ minus an accidental coincidence, depending on the distance from the center of an active zone.

Fit of an experimental dependence with the law $1/L^2$ is unsatisfactory, the goodness of such fit is only 12%. At a free parameter of the power fit, the best agreement with data is obtained with exponent -3.7.

Presence of fast neutrons from the reactor in a neutrino flux is supposed to be one of the most probable reasons for a deviation from the law $1/L^2$. One should notice, however, that in preparing an experiment, special measurements have been taken of a flux of fast neutrons at various distances to an active zone at the reactor On and Off in passive shielding [6]. The effect, associated with the reactor On, has not been observed. Results of measurements are presented in Fig. 6. The background form of fast neutrons is also determined by space radiation. The flux gradient of fast neutrons from the reactor is not found. However, the accuracy of the presented measurements is at the 10% level, and hence it is not yet sufficient to completely exclude the fast neutrons explanation of this deviation from the law $1/L^2$.

In order to decrease the influence of fast neutrons, the space (15 cm) between the reactor wall and passive shielding of the antineutrino detector has been filled with an iron pellet. The calculated factor of suppression of fast neutrons is about 3.

As pointed out in the introduction, along with observation of the spatial flux discrepancy, it is of significance to study a neutrino spectrum in various detector positions. This task requires conducting energy calibration of the detector. Before starting an experiment, a multi-section model was calibrated using γ -quanta source (^{22}Na) and a neutron source (Pu-Be). The results of energy calibration are presented in Fig.18. Removed active protection and the neutrino detector covers were calibrated by placing γ -quanta source (^{22}Na) and neutron source (Pu-Be) above the detector, irradiating in this way, practically, all sections. In a specific experiment with a separate section, there was studied dependence of ^{22}Na energy lines position on height .

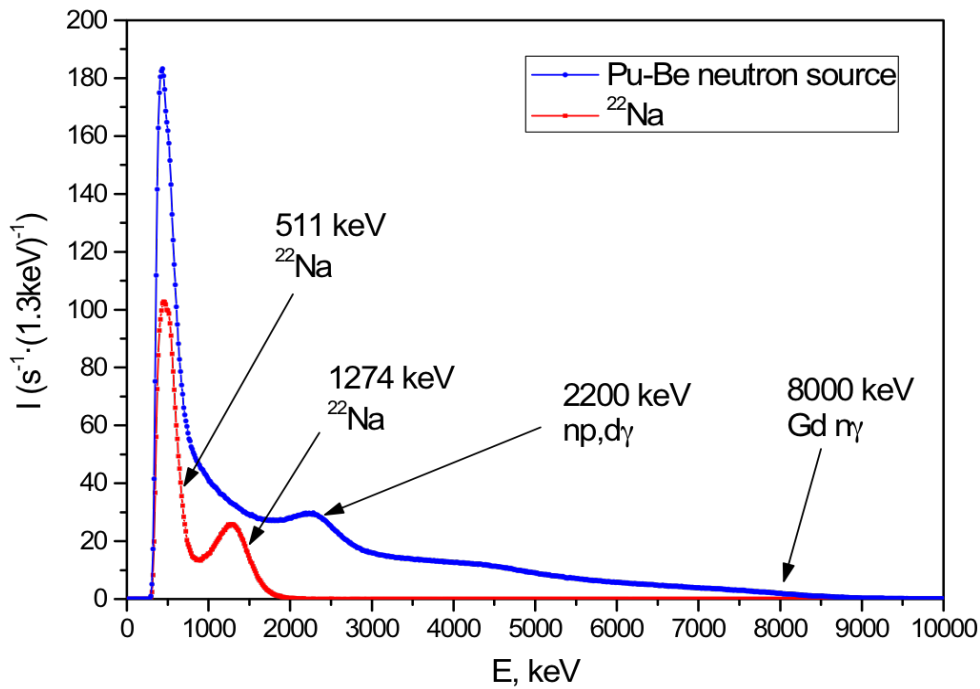


Fig. 18. Results of energy calibration.

9. Full-scale antineutrino detector.

The full-scale detector with a liquid scintillator has volume of 3m^3 (5×10 sections). The neutrino detector active shielding consists of external (“umbrella”) and internal parts regarding passive shielding. The internal active shielding is located on the top of the detector and under it.

In measurements with a full-scale detector, due to its sectional structure, we can use the same procedure with averaging efficiency of different cells.

The estimated probability of a start signal in the adjacent section, in which a major signal (bigger on amplitude) occurs, is 37.2% - an averaged value for all sections. Results of an experiment with probability of a starting signal in the adjacent sections are presented in fig. 19 for a differential signal of ON-OFF, and also for the reactor On and Off.

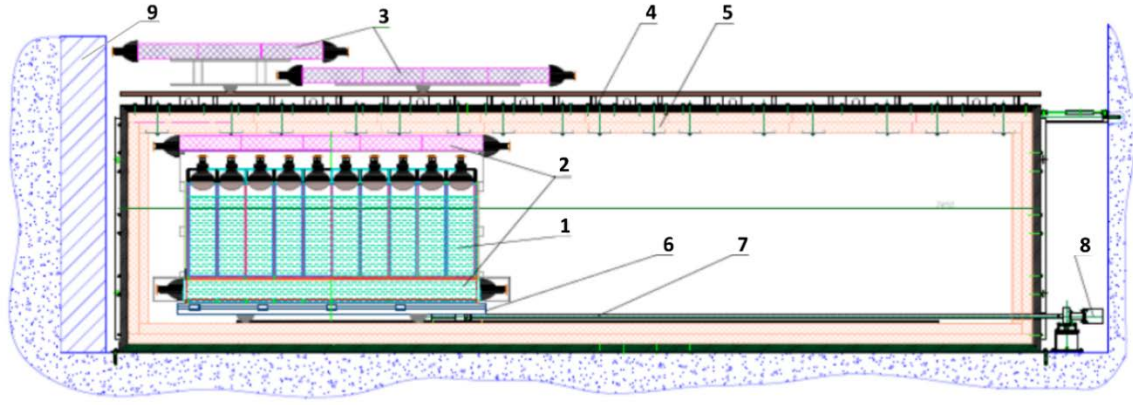


Fig 18. General scheme of an experimental setup. 1 – detector of reactor antineutrino, 2 – internal active shielding, 3 – external active shielding (umbrella), 4 – steel and lead passive shielding, 5 – borated polyethylene passive shielding, 6 – moveable platform, 7 – feed screw, 8 – step motor, 9 –shielding against fast neutrons from iron shot.

Table 1 shows probability estimations on positron events producing signals in two sections (with positron annihilated in the inner, side or corner section). For a full-scale detector, we use the first and the last rows of cells not for detecting a positron signal itself, but for annihilation gamma quanta at 511 keV. That means, that we have 16 side sections and 24 inner volume sections, with average probability for the full-scale detector to register multi-section signal from the positron event being 37.2%.

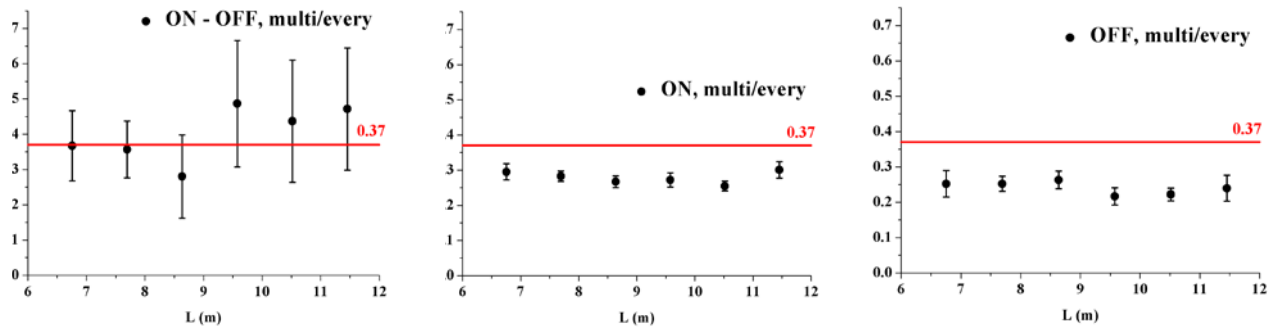


Fig. 19. Experimentally measured probability of a simultaneous starting signal in the adjacent sections for a differential signal of ON-OFF, and also for the reactor (ON) and (OFF).

Difference in parts of count rates at the reactor On and Off for double and single prompt events, integrated over all distances is $(37 \pm 4)\%$ and $(63 \pm 7)\%$. This ratio allows us to treat the recorded events as neutrino events.

Attempts to suppress the background of fast neutrons by sectioning the detector have yielded the required result. The relation effect/background was improved from 0.3 to 0.6. for a short distance from the detector to the reactor. Sectioning of the detector, as an additional selection criterion for neutrino events, has enabled to lower 2.5 times the background of an accidental coincidence, which negatively influenced the accuracy of measurements. Moreover, sectioning of the detector keeps off observing false effect of fast neutrons of the reactor. If such effect arises, it emerges mainly in the sections closest to the reactor.

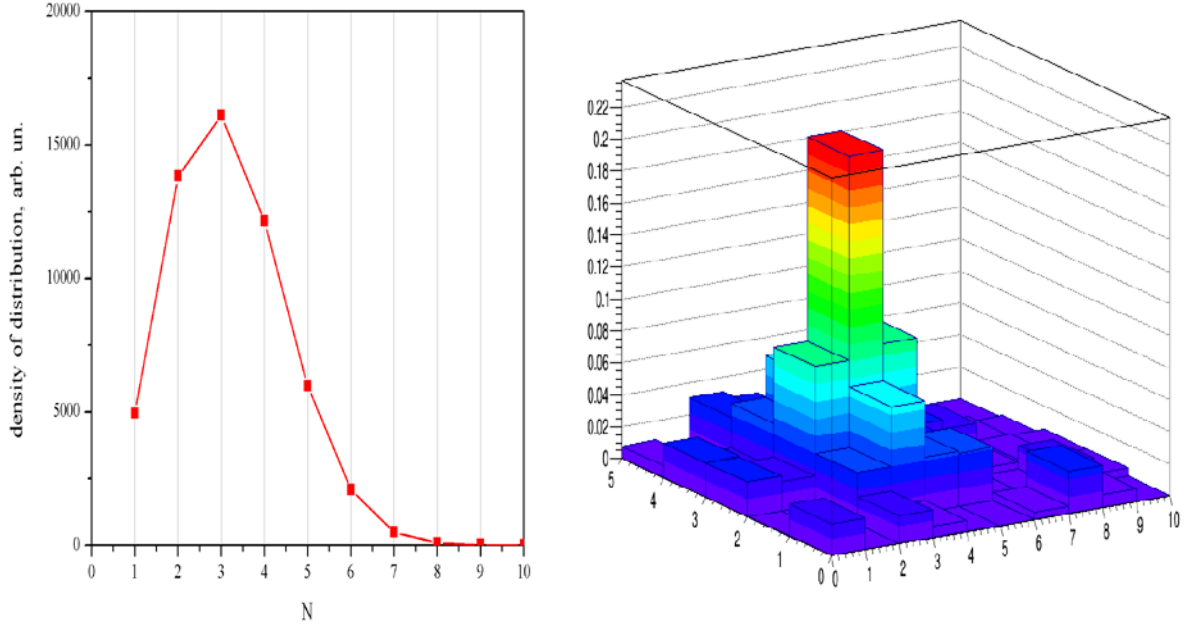


Fig. 20 a) Distribution of a neutron capture event in gadolinium over the quantity of involved sections, b) Distribution of delayed signals over the section (3, 3), in which a reaction of the inverse beta decay occurred .

10. Results of measurements.

Measurements by a full-scale detector with liquid scintillator volume of 3 m³ (5x10 sections) started in June, 2016. Measurements with the reactor ON were carried out for 196 days, and with the reactor OFF- for 107 days. In total, the reactor was switched on and off 25 times. First results of this work are presented.

Results of measurements on difference in counting rate of neutrino-like events for a full-scale detector are shown in fig.21, as dependence of antineutrino flux on the distance from the reactor center.

These data include only the measurements obtained on a full-scale detector. It is necessary to notice, that the previous publication [8] provided the data analysis with results from a detector model. Unfortunately, the article included some data, obtained before a gap between the reactor wall and the detector passive protection was filled with an iron pellet, which could bring about some effect of fast neutrons from the reactor. A new analysis is made only with data on a full-scale detector after iron pellet filling was applied, therefore the effect of fast neutrons from the reactor is completely excluded. Besides, the first and last rows of the detector are used as active protection, at the same time it can work as passive protection against fast neutrons.

Fit of an experimental dependence with the law $1/L^2$ yields not quite satisfactory result. The value of such a fit is slightly more than 10%, i.e. a deviation from the law $1/L^2$ can be observed at the confidence level of about 90%. At the same time, there is an experimental result of DANSS, kindly provided by M. V. Danilov, and also presented at the 52nd Rencontres de Moriond [9], which points out that in the range of 10 - 13 meters the law $1/L^2$ holds true with rather good accuracy. We can make use of this information and combine results of measurements in the range of their overlapping of 10 - 12 meters.

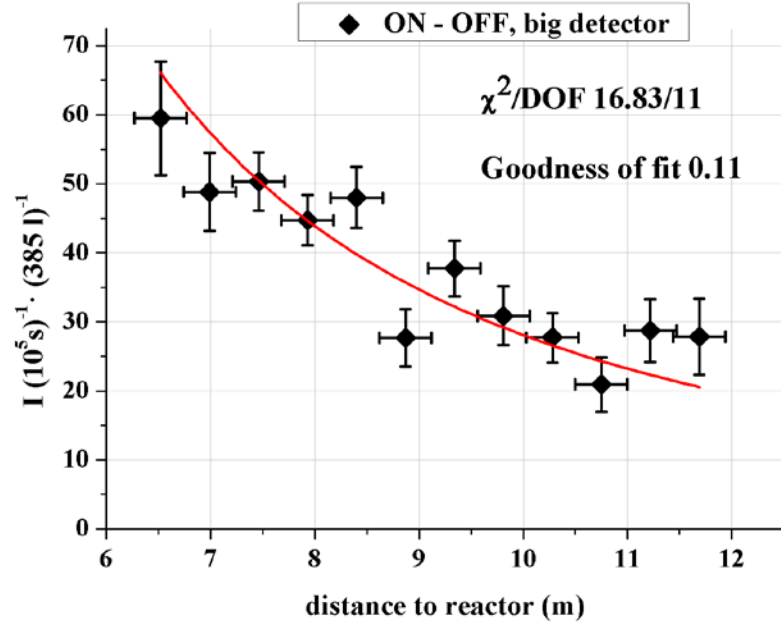


Fig 21. Reactor antineutrino flux distance dependence for a full-scale detector, the point graph fit for dependence of $1/L^2$, where L – distance from the center of reactor core.

Results of association of the Neutrino-4 and DANSS experiments data are presented in fig.22.

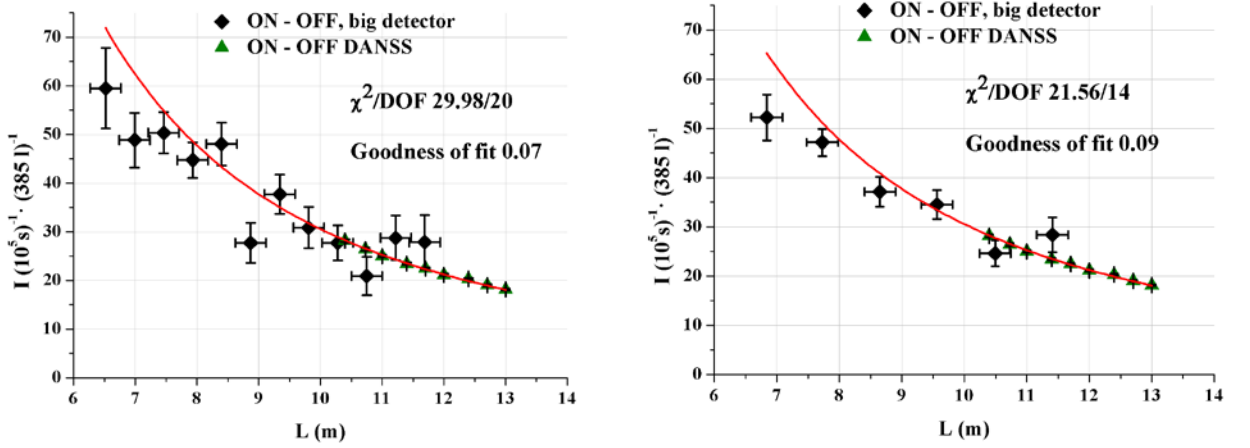


Fig. 22 Results of association of the Neutrino-4 and DANSS experiments data for dependence $1/L^2$. On the right, the same data on Neutrino-4 experiment are given, but averaged in the range of 1 meter.

It is of great interest to use the obtained experimental data of the Neutrino-4 and DANSS experiments for global fit of sterile neutrino model parameters. At the same time, it must be kept in mind, that at long distances results of fit should satisfy the results of measurements at these long distances. The obtained dependence and parameters of fit are presented in fig. 23. It should be noted, that the result of the analysis is very similar to the assumption from work [1].

The energy calibration for a full-scale detector was done in the same way as for a model detector. Results of calibration have been applied for measurement of a spectrum of prompt signals. The example of such measurements within one month is presented in fig. 24. Fig. 25 illustrates the spectrum of prompt signals summarized on all distances for the purpose of increasing statistical accuracy (averaged distance- 8.6 meters). This spectrum contains statistics of all measurements.

As both experiments in DANSS and in Neutrino-4 use relative measurements, it is necessary to mention, how points of DANSS become attached to Neutrino-4 points and are all together applied on an overall picture with results of other experiments. As shown in fig. 22, crossing of the DANSS and Neutrino-4 data is in the area of 10.5 – 11.5 m. At the same time, experimental data of DANSS are in good agreement with the law $1/L^2$. Therefore, the binding procedure is as follows: points of our experiment from the area of 10.5 – 11.5 m are laid down on the curve A/L^2 corresponding to DANSS points. It is reasonable to assume, that the errors of DANSS points must have been determined by an error of binding procedure (i.e. error at that point of the Neutrino-4, where the binding is carried out). As for the drawing points of DANSS and the Neutrino-4 in the picture of global fit, they are fixed so, that the curve of dependence is laid down on the average value defined as "reactor anomaly".

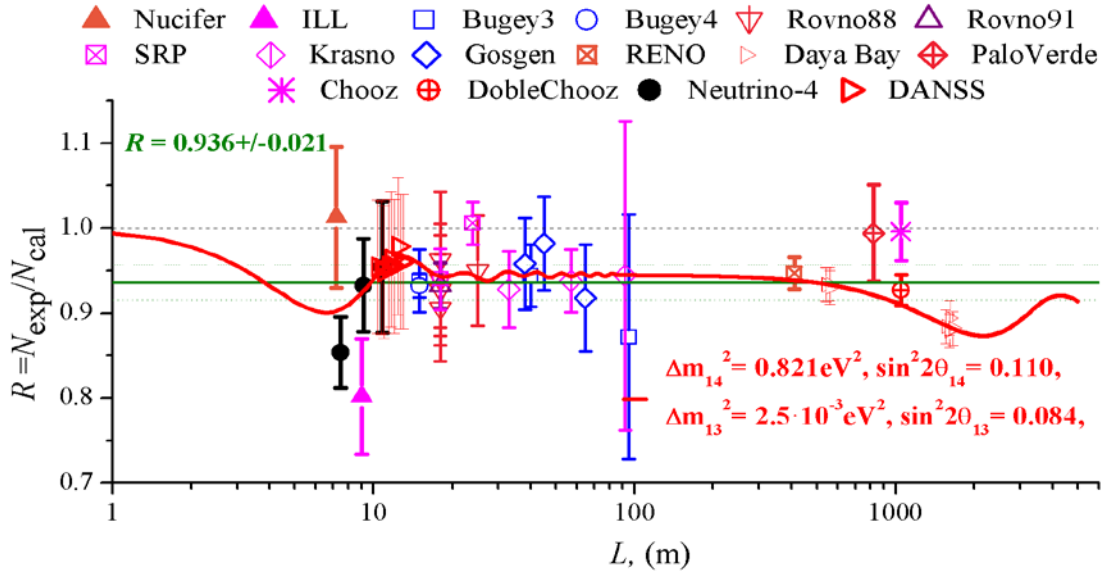


Fig. 23 Global fit of the sterile neutrino model parameters with experimental data of the Neutrino-4, DANSS and data of the known experiments at long distances [10,11]. The data of Neutrino-4 experiment are presented averaged in interval of measurements of 2 meters.

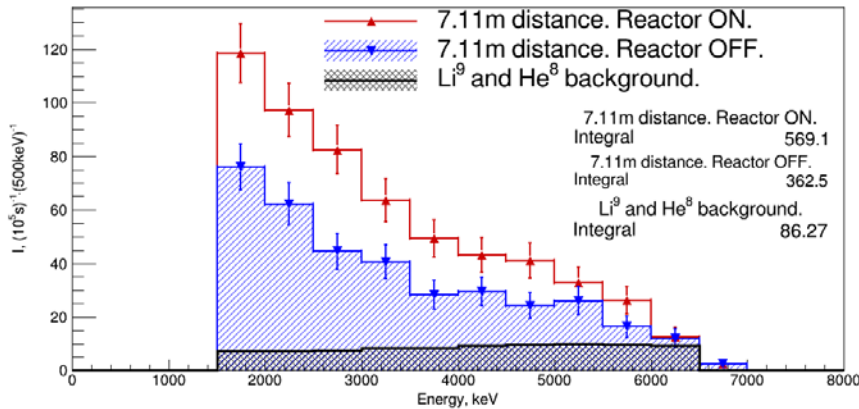


Fig. 24. Example of the spectrum of prompt signals obtained within one month of statistics. The signal (ON – OFF) has made 207 events per day. Relation effect/background (ON-OFF)/OFF = 0.57

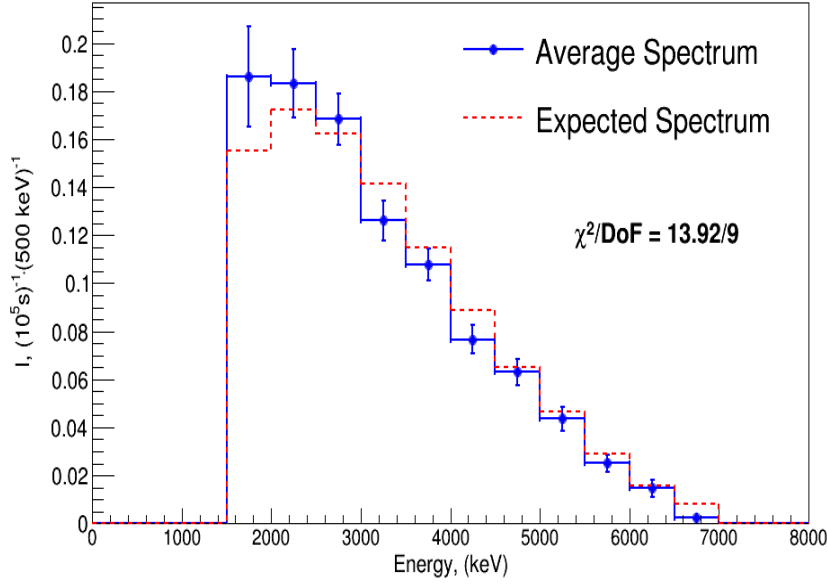


Fig. 25. Spectrum of prompt signals for a total cycle of measurements summarized on all distances (average distance - 8.6 meters). The red dotted line shows Monte Carlo simulation with neutrino spectrum for U^{235} , as the SM-3 reactor works on highly enriched uranium.

The ratio of an experimental spectrum of prompt signals to the spectrum expected from MC calculations is presented in fig. 26.

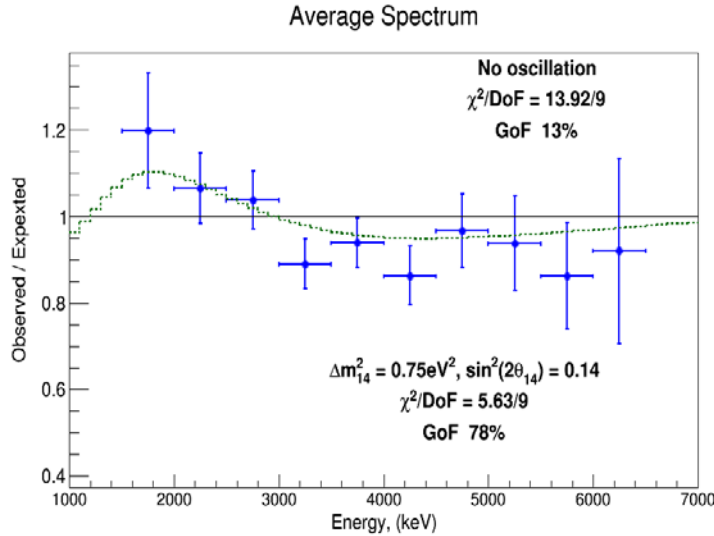
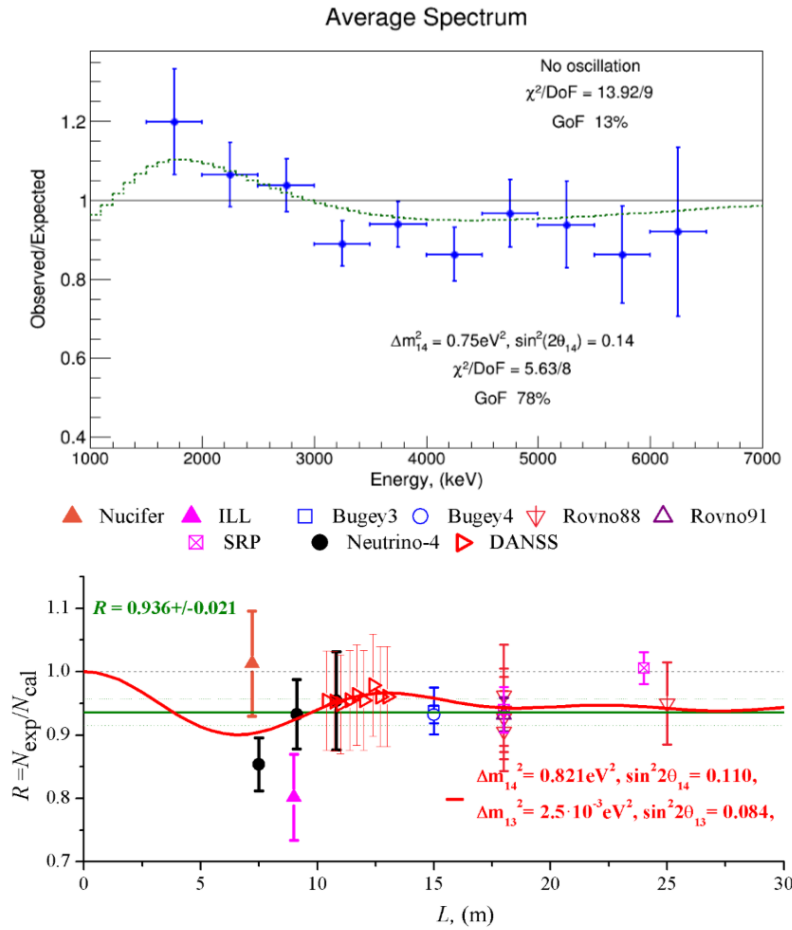


Fig. 26 The ratio of an experimental spectrum of prompt signals to the spectrum, expected from MK calculations.

Fit on the ratio without oscillations shows a low goodness of fit (13%), whereas fit on the assumed existence of oscillations with parameters $\Delta m_{14}^2 \approx 0.75 \text{ eV}^2$, $\sin^2 2\theta_{14} \approx 0.14$ gives the goodness of fit equals 78%. It is interesting to note, that parameters of oscillations Δm_{14}^2 and $\sin^2 2\theta_{14}$ for the analysis of spatial and energy distribution are identical. Of course, such a coincidence increases a magnitude value of the joint analysis, if it is not associated with possible systematic errors of an experiment. It should be noted, that measurements of spatial and energy distributions are practically independent. For descriptive reasons, results of both analyses are presented in Fig. 27.



$$\Delta m^2_{14} \approx 0.75 \text{eV}^2$$

$$\sin^2 2\theta_{14} \approx 0.14$$

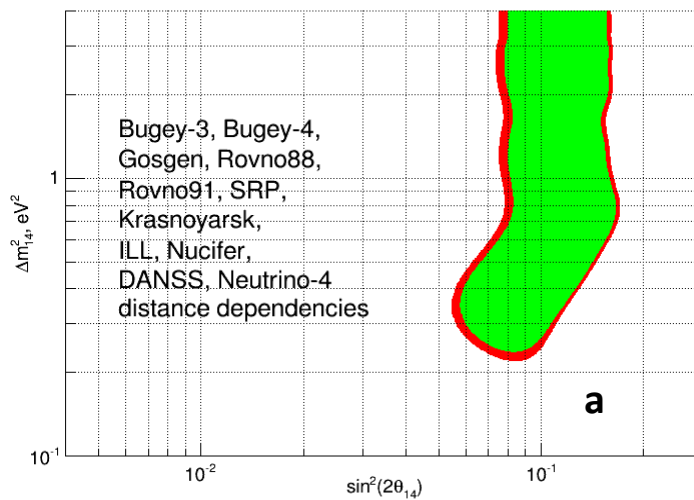
?!

$$\Delta m^2_{14} \approx 0.82 \text{eV}^2$$

$$\sin^2 2\theta_{14} \approx 0.11$$

Fig. 27. Analysis of experimental data on possible parameters of oscillations for spatial and energy distributions.

More detailed analysis of confidence level for parameters of oscillations Δm^2_{14} and $\sin^2 2\theta_{14}$ is also presented in Fig.29 by confidence level for spatial distribution, energy distribution and for the joint analysis of both distributions.



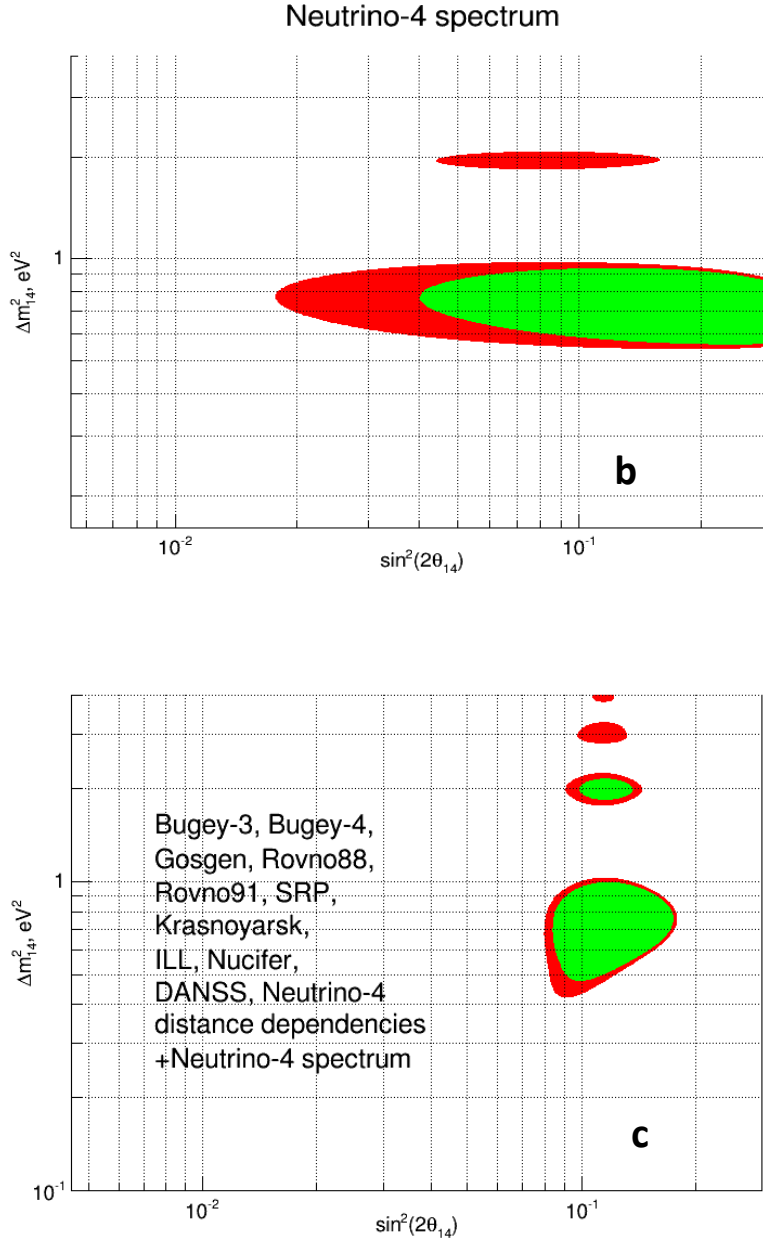


Fig. 28. Confidence Level (CL): a) for spatial distribution of data for experiments of the Neutrino-4, DANSS and other reactor experiments from [1] - b) for energy distribution of prompt signal of Neutrino-4 experiment and - c) for the joint analysis of power and spatial distributions. Green color corresponds to 95 – 98 % CL, red color corresponds to 98 – 99% CL.

12. Conclusion on the current experimental results and further prospects concerned with them.

Now it is necessary to make conclusions from the carried-out analysis of experimental data. First of all, it should be noted that the confidence level for a deviation of experimental data from the law $1/L^2$ is about 90%, i.e. 1.64 standard deviations. This level of confidence is obviously not enough for any conclusive statements. The similar situation arises in the spectral dependence analysis of prompt signals, of 90% level of confidence as well. The total analysis requires

identical parameters Δm_{14} and $\sin^2 2\Theta_{14}$, and up to 95% increase (2 standard deviations) in confidence level for possible existence of sterile neutrinos. However, it is not yet sufficient for making statements on observation of the phenomenon, especially as important as oscillations in a sterile state. Moreover, it is also unreasonable to exclude the possibility of influence of systematic errors on the final experimental result. The obtained result contradicts restrictions on parameters Δm_{14} and $\sin^2 2\Theta_{14}$, provided by experiments at Bugey-3[12], NEOS[13] and DANSS[9]. Therefore, we would like to concentrate our efforts on further enhancing accuracy of the experiment and controlling random systematic errors. Obviously, some increase in statistical accuracy is likely to be achieved, but it does not solve the problem in general.

The Neutrino-4 experiment started in 2014, at first on a model, then on a full-scale detector and, for the first time in the world, has provided measurement data on dependence of the reactor antineutrinos flux on the distance within 6 - 12 meters. Attempts to suppress the background of fast neutrons by means of sectioning the detector have given the required result. The effect/background ratio has been improved from 0.3 to 0.6. Sectioning of the detector on the criterion of an additional selection for neutrino events has allowed to lower an accidental coincidence background, negatively affecting the accuracy of measurements. Besides, sectioning of the detector makes it possible to keep off watching false effects from the reactor fast neutrons.

One of the principal problems, the Neutrino-4 experiment faced in making measurements on the SM-3 reactor, is the correlated background from fast neutrons induced by space radiation. It is caused by the fact that the building with an experimental installation is located on the Earth's surface and the concrete protection above the installation is not sufficiently thick.

Impact of accidental coincidence background on estimating accuracy can be decreased by raising gadolinium concentration in a liquid scintillator. It will allow to reduce the time window for a delayed signal from gadolinium gamma quanta to occur, thus diminishing probability of random coincidence. For the correlated background to be suppressed, it is necessary to involve the method of discriminating signals according to an impulse form, which enables to distinguish signals from heavy and light particles. For NEOS (Korea) experiment, one has elaborated and constructed a high quality scintillator capable of recognizing signals according to an impulse shape, which results in considerable lowering the level of the correlated background. Moreover, concentration of gadolinium in this scintillator is 5 times higher than that in our scintillator, which enables to decrease the background influence on an accidental coincidence.

Therefore, the first part of the project involves replacing the currently used scintillator with a new highly efficient one for discriminating signals according to an impulse shape, and with an increased concentration of gadolinium up to 0.5%. It is expected to reduce 3 times the accidental coincidence background as well as the correlated cosmic one, and to increase twice the current measurement precision.

The second part of the project is to create a new neutrino laboratory focused on solving essentially important problems outside the frame work of the current experiment:

- 1) monitoring of a cosmic background employing a double detector technique,

- 2) providing the required energy resolution for a detector by applying the double PMT technique on opposite sides of a scintillator,
- 3) performing calibration of the detector by using sources placed in the scintillator, thus enhancing the range of measurements up to 15 meters. The latter will provide an opportunity to carry out normalization of our data with the most accurate evidence obtained at 15 meter distance by Bugey-3 experiment.

In room No. 170, in the SM-3 reactor building, there is a place for a neutrino laboratory, in which it is possible to measure antineutrino flux within the range of 6 - 14 meters. The scheme of the installation is shown in fig. 29.

Neutrino laboratory on the SM-3 reactor in room №170

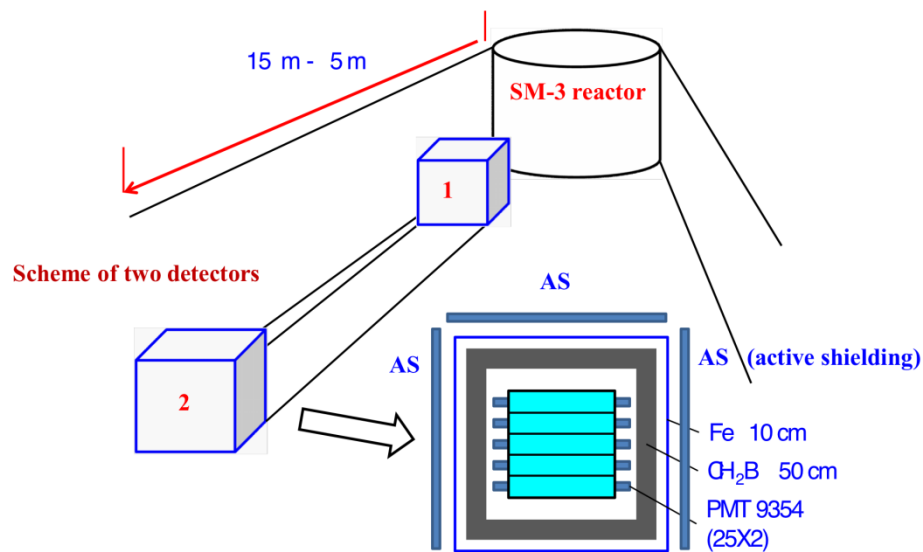


Fig. 29. Scheme of a new experiment on search for neutrino oscillations in room No. 170 of the SM-3 reactor.

In correspondence with a new project, two identical detectors are supposed to be used. One will be installed at maximum distance (15m) for a permanent operation, with the reactor antineutrino flux at this distance being rather weak, while the other will be moving from the first detector to the reactor. Passive and active shielding will be transported simultaneously with the second detector. The first detector is supposed to operate as a monitor, controlling change of the cosmic background. One also regards the option for applying a segmented detector, as shown in fig. 30. Besides, there is possibility of using a homogeneous scintillation volume by applying computer tomography for reconstruction of the event coordinates.

According to preliminary estimates, in two years of collecting data, we expect to obtain statistical accuracy at the level of 1-2% by measuring an antineutrino flux from the reactor. Thus, the problem of possible existence of a sterile neutrino with parameters in the range of $\Delta m_{14}^2 \approx 1eV^2$, $\sin^2 2\Theta_{14} \approx 0.1$ will be clarified.

In conclusion, it is necessary to notice that search for neutrino oscillations at small distances (6-12m) is to be performed on research reactors as well. Unfortunately, measurements should be taken in conditions of a considerable space background, and also in the conditions of much smaller neutrino flux. Nevertheless, carrying out measurements at small distances on research reactors is essentially important for a number of reasons. Research reactors operate on the enriched uranium, hence, uncertainty associated with a neutrino source range can be eliminated. The active zone of research reactors, as compared with a nuclear power plant, is not required to consider effects of burning out of fuel. Finally, effects of oscillations have been predicted at the distances of 6-12 m, so direct checking of oscillation effects is preferable and model independent. Moreover, an extended model with three sterile neutrinos requires detailed measurements at small distances. Now there is a number of projects on search for oscillations on research reactors (STEREO, SoLiD, PROSPECT), therefore it is possible that the problem of a space background will be solved and this area of distances will be explored.

Acknowledgments

The authors are grateful to the Russian Foundation of Basic Research for support under Contract No. 14-22-03055-ofi_m. The delivery of the scintillator from the laboratory headed by Prof. Jun Cao (Institute of High Energy Physics, Beijing, China) has made a considerable contribution to this research.

References

- [1] T. Mueller, D. Lhuillier, M. Fallot et al., Phys. Rev. C 83, 054615 (2011).
- [2] G. Mention, M. Fehner, Th. Lasserre et al., Phys. Rev. D 83, 073006 (2011).
- [3] A. P. Serebrov, A. K. Fomin, V. G. Zinoviev et al., Tech. Phys. Lett. 39, 636 (2013); arXiv:1205.2955
- [4] A. P. Serebrov, A. K. Fomin, V. G. Zinoviev et al., Tech. Phys. Lett. 40, 456 (2014); arXiv:1310.5521
- [5] A. P. Serebrov, V. G. Ivochkin, R. M. Samoilov et al., Tech. Phys. 60, 1863 (2015); arXiv:1501.04740
- [6] A. P. Serebrov, V. G. Ivochkin, R. M. Samoilov et al., JETP 121, 578 (2015); arXiv:1501.04740
- [7] A. P. Serebrov, V. G. Ivochkin, R. M. Samoilov et al., Tech. Phys. 62, 322 (2017); arXiv:1605.05909
- [8] A. P. Serebrov, V. G. Ivochkin, R. M. Samoilov et al., JETP Lett. 105 (6), 329 (2017); arXiv:1702.00941
- [9] M. V. Danilov The 52nd Rencontres de Moriond Electroweak Interactions and Unified Theories, March 24, 2017, Thuile, <https://goo.gl/c8WUsV>
- [10] C. Giunti, Neutrino 2016 XXVII International Conference on Neutrino Physics and Astrophysics 4 – 9 July 2016, London, UK, <https://goo.gl/v1WrUi>
- [11] Yu-Feng Li, Applied Anti-neutrino Physics 2016, 1 – 2 December, University of Liverpool, Merseyside, UK, <https://goo.gl/m2OJlj>
- [12] B. Achkar, R. Aleksan, M. Avenier et al., Nucl. Phys. B 434, 503-532 (1995)
- [13] Y. J. Ko, B. R. Kim, J. Y. Kim, et al., Phys. Rev. Lett 118, 121802 (2017)